*Larhyss Journal, ISSN 1112-3680, n°28, Dec 2016, pp. 219-235*


# EFFECT OF RIVER INFLOW ON WATER QUALITY RESERVOIRS STUDY CASE 'SAU RESERVOIR'

## EFFET D'ECOULEMENT GES EAUX DE RIVIERE SUR LA QUALITEE DES EAUX DANS LES RESERVOIRS (CAS ETUDIE RESERVOIR SAU)

***TAKKOUK S.[1], CASAMITJANA X.[2], BOUGUERNE A.[3]***

[1] Département d'hydraulique, Faculté de Technologie, Université de Batna, Algérie.
[2] Département de Physique, Université de Gérone, catalogne, Espagne
[3] Département d'hydraulique, Faculté de Technologie, Université de Batna, Algérie.

*takkouks@yahoo.com*

## ABSTRACT

The aim of this work is to apply 3D hydrodynamic model ELCOM (Estuary and Lake Computer Model), combined with water quality model CAEDYM (Conceptual aquatic environment dynamic) model to Sau reservoir. This study is an attempt to get an idea about the effect of river water inflow dynamic on water quality in daily time scale. Simulation takes place in summer period in stratified conditions and has been undertaken for approximately one week starting in the end of July of the 2005. This, study may contribute for future investigation and environmental consequences of water quality in Algerian Reservoirs.

**Key-words:** Hydrodynamic, dissolved oxygen, water quality.

## RESUME

Le but de ce travail est d'appliquer un modèle hydrodynamique en trois dimensions (3D) ELCOM (Estuary and Lake Computer Model) en combinaison avec un modèle de qualité d'eau CAEDYM (Conceptual aquatic environment dynamic) pour un réservoir Sau situé en catatonie (Espagne). Cette étude est un essaye d'avoir une idée sur l'influence du mouvement des eaux de la rivière Ter

en entrant dans le réservoir sur les qualités de l'eau. Les simulations ont été prise lors de la période de stratification approximativement une semaine débutant à la fin de juillet. Cependant, cette étude peut contribuer pour des futures recherches à savoir les conséquences environnementales dues à la qualité des eaux dans les réservoirs algériens

**Mots-cles:** Hydrodynamique, oxygène dissout, qualité des eaux.

## INTRODUCTION

It is very common for water flowing into reservoirs to be either denser or less dense than the receiving water. These density differences can result from temperature variations or different suspended or dissolved solids concentrations.

When water of higher density flows into an ambient water body of lower density a plunging inflow is produced. As the denser water flows into the ambient body of water, it pushes the lighter, ambient fluid ahead (Akiyama and Stefan, 1984). The buoyancy force generated by pushing the lighter water back into the reservoir retards the momentum of the inflowing water. Eventually the momentum of the inflowing water is reduced to the point that its excess gravitational attraction becomes dominant and the denser water then plunges beneath the surface of the ambient water and finally flows as a density current along the inclined bottom of the reservoir. The water will flow along the bottom as a density current downward to the level of neutral buoyancy or to the bottom of the basin. Neutral buoyancy occurs when the densities of the flowing current and the ambient fluid at the depth of the flowing current are equal. At that time the density current will separate from the bottom and insert itself into the body of the ambient water. The review article by (Alavian et al, 1992) provides a good description of the processes.

Entrainment and mixing of the ambient water into the dense, inflowing water stream occurs both in the region of the plunge and after the flow has assumed the form of a density current. Processes of entrainment into density currents are well suited to laboratory studies and have been studied extensively for comparatively simple cases, (Savage and Brimberg, 1975) and (Akiyama and Stefan, 1984). Entrainment and mixing within the plunge zone has received less attention, although it is estimated that up to 80% of the total entrainment can occur in the plunge, (Ford and Johnson, 1983).

Sau reservoir is river valley reservoir (Fig.1) receiving water from Ter river inflow.

Sau Ter Inflow dynamic has been investigated by a team leaded by (Armengol et al, 1994) of the university of Barcelona to see how river Ter behaves when enters Sau reservoir. So this team has studied the long term longitudinal processes associated with the river circulation in the Sau reservoir. In winter, the inflow temperature is lower than that of the reservoir resulting in an underflow. This deep flow continues until February, when the river temperature rises faster than the surface water of the reservoir, resulting in an overflow. From February to April-May, the surface flow corresponds to the start of the spring phytoplankton bloom due to the introduction of nutrients into the photic zone. The transition between spring and summer is characterized by an interflow that sinks progressively until mid November when it reaches the bottom as an underflow.

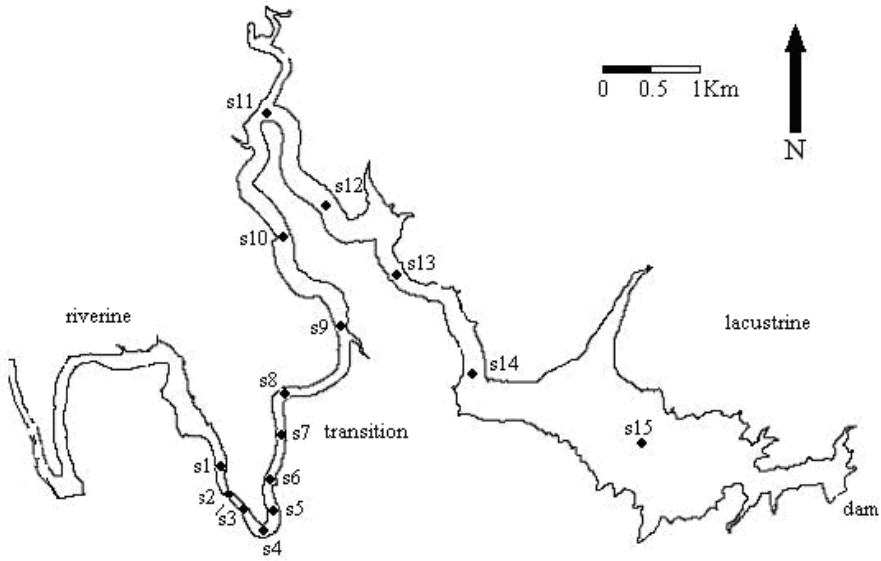


**Figure 1 : Situation of the measuring stations along the Sau Reservoir. The reservoir has been divided into riverine, transition and lacustrine zones.**

## 2. MATERIAL AND METHODS

The data used here was obtained during a field campaign carried out during the summer period started from 26$^{th}$ July to the 3$^{rd}$ August, 2005 (207-215 Julian days). Meteorological data that was supplied from a nearby automatic station in the river Ter and from the station placed in the lacustrine part of the reservoir

(Fig.1). Temperature and nutrients in the river were obtained from an automatic station located approximately 5 km upriver. Temperature, inflow outflow, and phosphorous, dissolved oxygen are displayed in Fig. 3.

## NUMERICAL MODELLING

Numerical model used here is 3D hydrodynamic model ELCOM which was developed in the Water Research Centre of the University of Western Australia. (Laval, and Hodges, 2000), (Hodges, 2000) and (Hodges and Dallimore, 2006). ELCOM is used for predicting the spatial and temporal distributions of temperature, density and salinity.

Ecological model CAEDYM (Hipsey et al, 2005) and (Schladow, et Hamilton, 1997) is a water quality model that can simulate the dissolved oxygen, nutrients and chlorophyll, in the reservoirs, when is combined with the hydrodynamic 3D ELCOM. In Sau reservoir ELCOM-CAEDYM was configured to simulate only one phytoplankton group which is cyanobacteria (Fig. 2), together with, phosphorus and oxygen dynamics. CAEDYM was the same model used on combination with 1D Dynamic Reservoir simulation model DYRESM to simulate temperature dissolved oxygen, phosphorus and phytoplankton in Sau reservoir (Romero et al, 2007) and (Takkouk et al, 2015).

The main equations used in CAEDYM for dissolved oxygen, phosphorous and chlorophyll are shown in Table 1. CAEDYM

The simulated period is 05 days starting from the day 206.5 of the year 2005. Our goal is to understand how the spatial and temporal evolution of dissolved oxygen, phytoplankton and nutrients due to the river dynamic. It is well known that certain algal blooms may be harmful especially in reservoirs that could be transported in water and might be used for supplying drinking water to inhabitants. As the initial concentrations, for the dissolved oxygen, dissolved inorganic phosphorous, chlorophyll were unknown, we only try to know how dissolved oxygen, phosphorus and chlorophyll will respond to a highly dynamic system. Also, we will evaluate the ecological response of the model to the inflow dynamics. The main parameters used in the model are summarized in Table 2

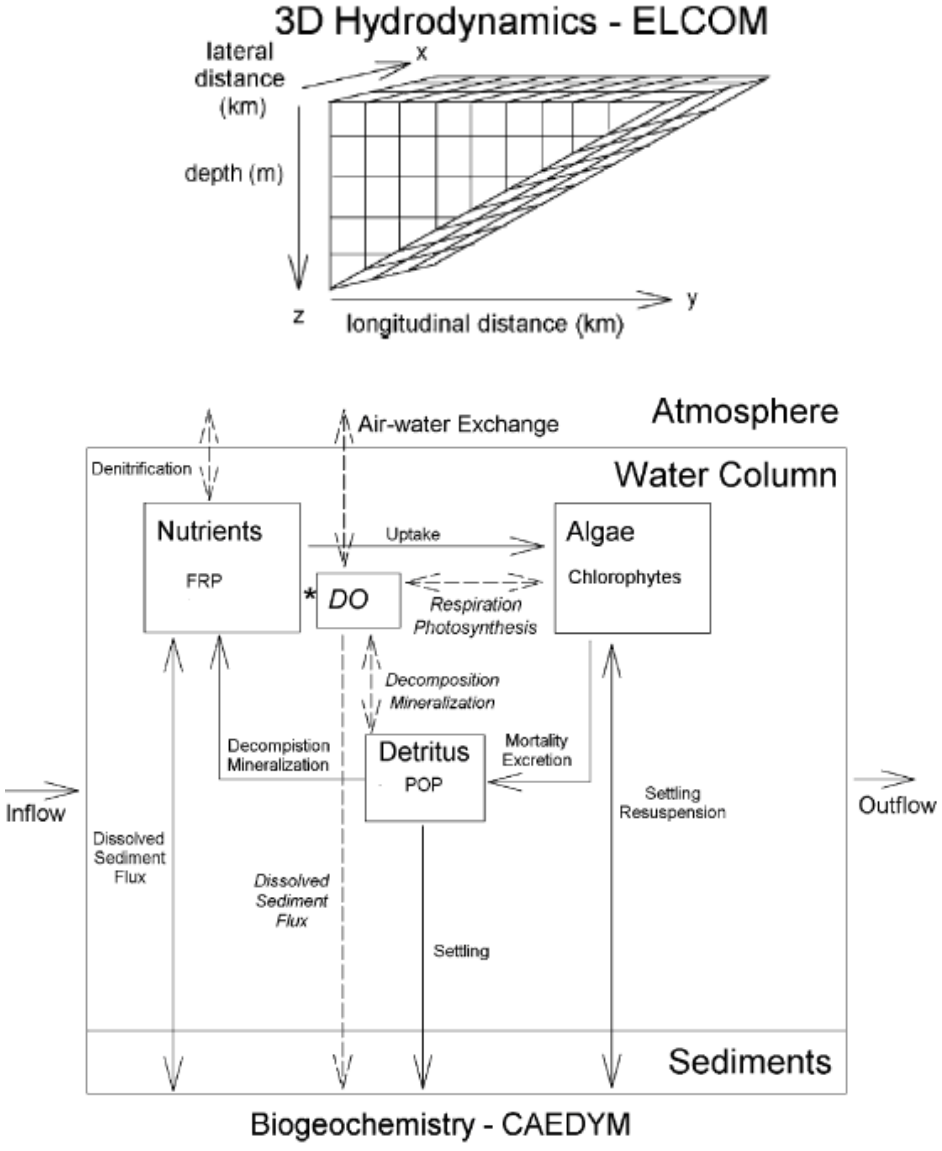


**Figure 2 : Hydrodynamic model ELCOM combined with water quality CAEDYM model**

**Table 1 : Main equations used in CAEDYM**

Dissolved oxygen

$$\frac{\partial \mathrm{DO}}{\partial t} = \underbrace{k_a(\mathrm{O_a} - \mathrm{DO_w})}_{\text{air–water flux}} + \underbrace{\sum_{i}^{D,G,B} \{\mu_i(1-k_p) - k_{ri} f(T)\} Y_{O:C} Y_{C:chla} A_i}_{\text{algal oxygen consumption/production}} - \underbrace{f(C_{DO})}_{\text{mineral}} - \underbrace{k_n f(T) \frac{\mathrm{DO}}{K_n + \mathrm{DO}} \mathrm{NH_4}^+ Y_{O:N}}_{\text{nitrification}}$$

$$- \underbrace{\frac{f(T) F_{SOD} \mathrm{DO}/(\mathrm{DO} + K_{SOD})}{h}}_{\text{sediment oxygen demand}}$$

Phosphorus

$$\frac{\partial \mathrm{FRP}}{\partial t} = \underbrace{-\sum_{i}^{D,G,B} \mu_i Y_{P:chla} A_i}_{\text{algal FRP uptake}} + \underbrace{\left\{\left[\frac{k_{AP} K_{OP} + k_{OP}\mathrm{DO}}{K_{OP} + \mathrm{DO}}\right] f(T)\mathrm{POP}\right\}}_{\text{organic matter mineralization}} + \underbrace{\frac{f(T) S_P K_{DOS}/(K_{DOS} + \mathrm{DO})}{h}}_{\text{dissolved sediment flux}}$$

$$\frac{\partial \mathrm{POP}}{\partial t} = \underbrace{\frac{v_P}{\Delta z}\mathrm{POP}}_{\text{settling}} - \underbrace{\left\{\left[\frac{k_{AP} K_{OP} + k_{OP}\mathrm{DO}}{K_{OP} + \mathrm{DO}}\right] f(T)\mathrm{POP}\right\}}_{\text{organic matter mineralization}} + \underbrace{\sum_{i}^{D,G,B} k_r f(T) Y_{P:chla} A_i}_{\text{mortality and excretion}}$$

Phytoplankton group $A_i$ where $i$ = D for diatoms, $i$ = G for green algae and $i$ = B for blue-green algae

$$\frac{\partial A_i}{\partial t} = \left\{ \underbrace{\mu_i}_{\text{growth}} - \underbrace{k_{ri} f(T)}_{\text{respiration}} + \underbrace{\frac{v_i}{\Delta z}}_{\text{settling}} \right\} A_i + \underbrace{\frac{\alpha_A(\tau - \tau_{cA})/\tau_r A_{imass}/(A_{imass} + K_{imass})}{h}}_{\text{resuspension}}$$

$$\mu_i = f_i(T)\mu_{maxi}\min[f(I), f(N), f(P)] \qquad f_i(T) = \theta^{T-20} + \theta^{k(T-a)} + b$$

$$f(P) = \frac{\mathrm{FRP}}{\mathrm{FRP} + K_{Pi}} \quad f(N) = \frac{\mathrm{NH_4}^+ + \mathrm{NO_3}^-}{\mathrm{NH_4}^+ + \mathrm{NO_3}^- + K_{Ni}} \quad f(I) = 1 - \exp\left(-\frac{I}{I_K}\right) \quad f(T) = \theta^{T-20}$$

The hydrodynamic model ELCOM was run using a uniform horizontal 20 x 20m grid, with a previously straightened bathymetry (Hodges et al, 2000) and (Imberger, 2001). Different cell sizes were used in the vertical plane with high resolution (0.25m cells) in the first few meters and increasingly lower resolution (up to 1m cells) in the deeper layers.

**Table 2 : Main parameters used in CAEDYM**

| Parameter | Value | Description |
|---|---|---|
| | | Dissolved Oxygen |
| *FSOD* | 0.32 | Static DO consumption by sediments (gDOm2 per day) |
| *KDOS* | 0.5 | DO 1/2 saturation constant for sediment oxygen demand (mgDOl−1) |
| | | Dissolved Inorganic Carbon |
| *YP:chla* | 0.3 | Fixed algal P to chla ratio (mg P (mg chla)−1) |
| *kOP* | 0.010 | Aerobic POP mineralization rate (per day) |
| *kAP* | 0.003 | Anaerobic POP mineralization rate (per day) |
| *vP* | -0.1 | Settling velocity of POP (m per day) |
| *SP* | 0.005 | Maximum FRP sediment flux (g Pm−2 per day) |
| *KOP* | 5.0 | DO 1/2 saturation constant for POP mineralization (mgDOl−1) |
| | | Chlorophyll |
| *Kri* | 0.08 | Respiration rate coefficient (per day) |
| *vi* | -0.01 | Algal settling velocities (m per day) |
| *μi* | 1.2 | Maximum specific growth rate at 20 °C (per day) |
| *θ* | 1.08 | Temperature multiplier for temperature limitation of phytoplankton growth |
| *k* | 2.19 | Coefficient for temperature limitation function for phytoplankton (dimensionless) |
| *a* | 30.05 | Coefficient for temperature limitation function for phytoplankton (dimensionless) |
| *b* | 0.182 | Coefficient for temperature limitation function for phytoplankton (dimensionless) |
| *Kpi* | 6 | Half-saturation constant for phosphorus uptake (mg m-3) |
| *Kni* | 30 | Half-saturation constant for nitrogen uptake (mg m-3) |
| *Iki* | 500 | Irradiance parameter for non-photoinhibited phytoplankton growth (μEm-2 s-1) |

## 4. SIMULATION AND RESULTS

The inflow dynamics is governed by the density difference between the river and the reservoir, while temperature is usually the main factor controlling density. The river temperature is highly dependent on the air temperature, quickly responding to short term variations in the latter (Fig. 3A). During the survey, the river inflow was around 2 to 3 $m^3$ $s^{-1}$ (Fig. 3B) and the outflow, which was intermittent, was normally higher than the inflow so the water level was decreasing throughout the survey. Phosphorous, is usually the limiting factor of the algal growth in Sau (Armengol et al. 1999) was increasing and

decreasing throughout the survey period and is showed in Fig 3C. The average dissolved oxygen concentration is 5mg/l is displayed in Fig 3D.

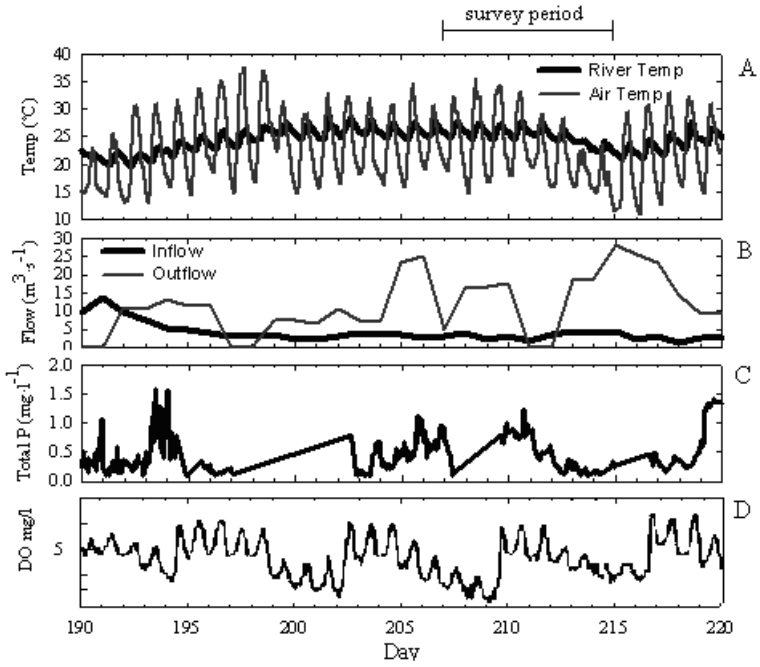


**Figure 3 : Evolution of (A) river temperature and air temperature from Julian day 190 (2005) till 220 (2005). (B): inflow and outflow, (D): concentration of total phosphorus in the river and (E): dissolved oxygen concentration in the river**

## DESCRIPTION OF DYNAMICS

Survey period has been taken in stratification period, thus last days of July 2005 were quite warm days, as can be seen in Fig 3A. The dynamics of the river inflow into the reservoir were mainly influenced by the temperature variation. Fig. 3A shows that the response time of the river temperature to changes in air temperature is very short and occurs at different time scales, from daily to longer periods. Also, as the response of the river temperature is faster than the ambient reservoir water, the river insertion into the reservoir alternated between overflow and interflow, depending essentially on the inflow rate, ambient water stratification and inflow temperature. As the day went on, the river became warmer, eventually reaching temperatures similar to those of the surface water of the reservoir, it separates from the bottom and flows up and over the surface

of the ambient water thus generating an overflow (Fig. 4A) in the afternoon and early in the night. However, during the night, the river became colder than the water surface and eventually, late in the night and morning inflowing waters that have a higher density than the ambient water, the inflowing water plunges under the surface to form underflow, the plunge flow region is momentum dominated. After the plunge occurs the density current becomes buoyancy dominated if the inflow momentum is large enough to displace the ambient water horizontally over the entire depth of the lake. At the "plunge point," the baroclinic force resulting from the inflow/ambient density difference balances the inflow momentum, so the inflow plunges beneath the ambient water. In the "plunge region" close to the plunge point, both the flow momentum and baroclinic forces affect the flow dynamics. In the "underflow region" the flow is entirely baroclinic and is therefore independent of inflow momentum. Ellison and Turner (1959) showed that after plunging the underflow quickly reaches a normal state where the bulk Richardson number is constant. The "plunge depth" is therefore the depth where the inflow moves from momentum-dominated to buoyancy-dominated and marks the transition of an inflow to an underflow Fig.4B

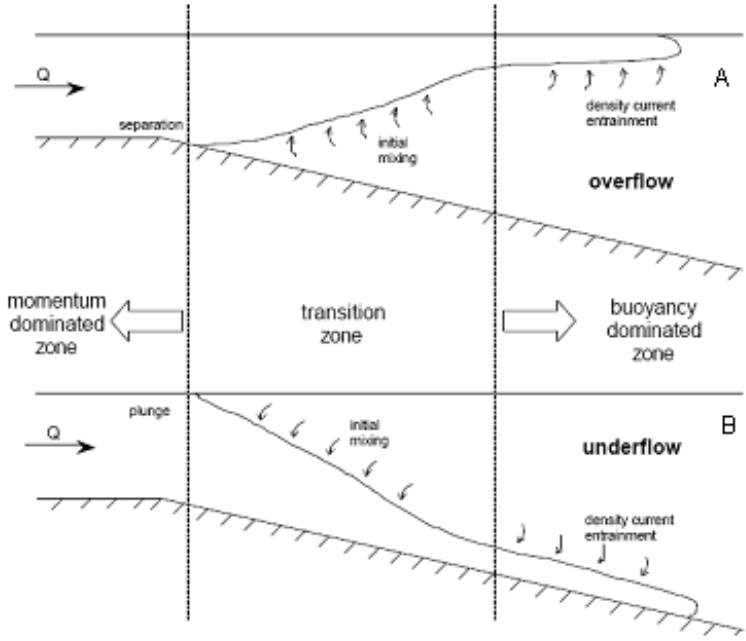


**Figure 4 : Definition of (A) overflow and (B) underflow regimes.**

Whether lifting off from the bottom or plunging from the surface, a certain volume of ambient water entrained in the transition zone between a momentum dominated flow and a buoyancy-dominated flow. Entrainment of ambient water into the inflow during this transition will be designated “initial or inflow mixing” to differentiate it from the entrainment in the subsequent buoyancy dominated region of the overflow or underflow density current.

When the interflow occurred, the temperature of the river was lower than the ambient surface temperature and the inflow plunged at about 1000m from station s1 (Fig. 5). Then, the inflow behaved as an underflow until at approximately 6m depth and 4000 m length, until reach the insertion point. The Chlorophyll-a values (Fig.6D) are characterized by three main peaks. The first one is clearly located in the plunge zone where the river converges with the ambient water and the accumulation of matter from the ambient water, including phytoplankton, is expected. Part of this Chlorophyll entrains into the inflow and is dragged to the bottom, as can be seen in Fig. 6D. The second peak, with values of more than 40 mg/m3, is located at around 6000-7000m distance coinciding with the head of the overflow events and the third peak situated at station 14 at the beginning of lacustrine zone. Latter on we will see how dynamic inflow variability can generate physical and biological consequences.

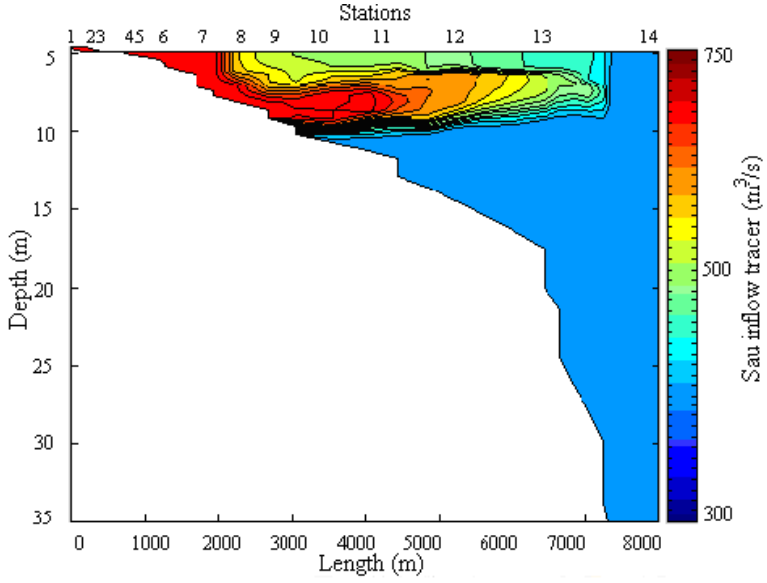


**Figure 5 : Longitudinal contours of salinity following the thalweg during day 211 of Sau inflow tracer**

## PHYSICAL EFFECTS

Rivers may introduce nutrients, suspended sediments, and contaminants into reservoir. A dense river inflow that penetrates to the hypolimnion of a lake will have different ecological consequences. One of the consequences is the entrainment which leads to an increase of hypolimnetic temperatures in reservoirs, since the cooler inflow water entrains the warmer ambient water and leads to baroclinic forces affecting the flow structure. Similarly, the fate of a dissolved or suspended contaminant being carried with the original inflow, or contained in the surface layer of the reservoir, is dependent on entrainment. Entrainment might be great enough to dilute the contaminant and render it harmless, or it could be so little as to insert and confine the contaminant within a narrow layer in the reservoir. The contaminant can be quickly transported through the reservoir if the level of insertion is at the same level as an outflow; or it can remain trapped by stratification for an extended period if insertion is at a level not influenced by the outflows.

Thus, understanding of how the inflow mixes with and merges into the reservoir is crucial in understanding how nutrients or any possible contaminants will be distributed or diluted throughout the reservoir. In recent years, a great deal of effort has gone into determining the inflow entrainment coefficients (Dallimore, 2001), (Hebbert et al, 1979) , (Ellison & Turner, 1959) and (Atkinson, 1988).

In the case of the Sau reservoir, inflow is highly variable depends on the precipitation and catchments area characteristics for this case as shown in Fig. 3B inflow was approximately constant and might be originate from snow melting from preneu mountains.

## BIOLOGICAL EFFECTS

From a water quality point of view, inflow dynamic is necessary for predicting the spatial and temporal distributions of temperature, dissolved oxygen, nutrients, pollutants, and sedimentation that rivers provide to a reservoir. Thus, it is important to know how the river nutrients will be distributed along the reservoir and the effect of such nutrients over the phytoplankton populations. (Armengol et al, 1999) and (Comerma, 2003) described the longitudinal differences in the nutrient distribution in the reservoir. As the input of nutrients from the river Ter is high, it is important to know how they will be distributed throughout the reservoir, in order to be able to predict the phytoplankton evolution. The oscillating dynamics of the inflow mean that new nutrients are

injected everyday into the reservoir surface. When the injected water, rich in nutrients encounters the eutrophic reservoir water rich in phytoplankton, conditions for phytoplankton growth are excellent. The explanation of the progression or evolution of the river and the head of the injected overflows is illustrated in (Fig. 5) where the inflow tracer enters to the reservoir. A bloom of phytoplankton located around station S9 (3 km) at the head of the injected overflowing water can be appreciated in Fig. 6D. On day 211 at station 9 simulated Temperature was (30C°) (Fig. 6A), concentrations of dissolved oxygen was (6 mg/L) (Fig. 6B) and dissolved phosphorus was (0.5 mg/L) (Fig. 6C), theses concentrations were favourable to the formation of the algal bloom. Algal blooms in zones with high nutrient concentration were found and these were related to the hydrodynamics of the river inflow. Therefore, our understanding of the coupling between the inflow physics and the biological processes was clearly enhanced.

In Fig 3A the dissolved oxygen of water river on the day 211 is about (5mg/l) this low concentration might be due to the fact that the river water is very poluted upstream station 9 In Fig. 6B the dissolved oxygen concentration is similar as the river (6 mg/l) on the same simulated day 211at station 9 where the inflow concentration of dissolved nutrient was high enough for the algal growth.

The concentration of the bloom on the day 211 (Fig. 6D) is about (50 mg/m$^3$) is the maximum concentration at station 14 corresponding to the high simulated temperature (Fig 6A), high dissolved oxygen (Fig. 6B), and increase in phosphorus concentration (Fig. 6C).

Simulations started on day 206.5. (Fig. 7) show a successive three-day (208, 209, and 210) evolution of dissolved oxygen, total phosphorus, and chlorophyll. It can be seen how the model is able to reproduce the overflow and interflow fluctuation and how inflowing water, rich in phosphorous, and poor in dissolved oxygen is injected at the surface and at the insertion depth. Therefore On day 208 (Fig 7A, 7B, and 7C)) the head of the surface overflow and the head of the interflow (at a depth of approximately 4m) are clearly seen. As the inflow evolves, from day 206.5 to day 210) the overflow head had travelled a distance of about 4 km while the interflow head slowly advanced towards the dam (Fig 7). Also, algal blooms are generated where the head of the overflow is located, it is important to point out that the bloom was formed where the water from the river rich in nutrients encountered the water from the reservoir rich in phytoplankton). Therefore, the model is able to predict the bloom observed in the field survey (Fig. 6 and Fig. 7).

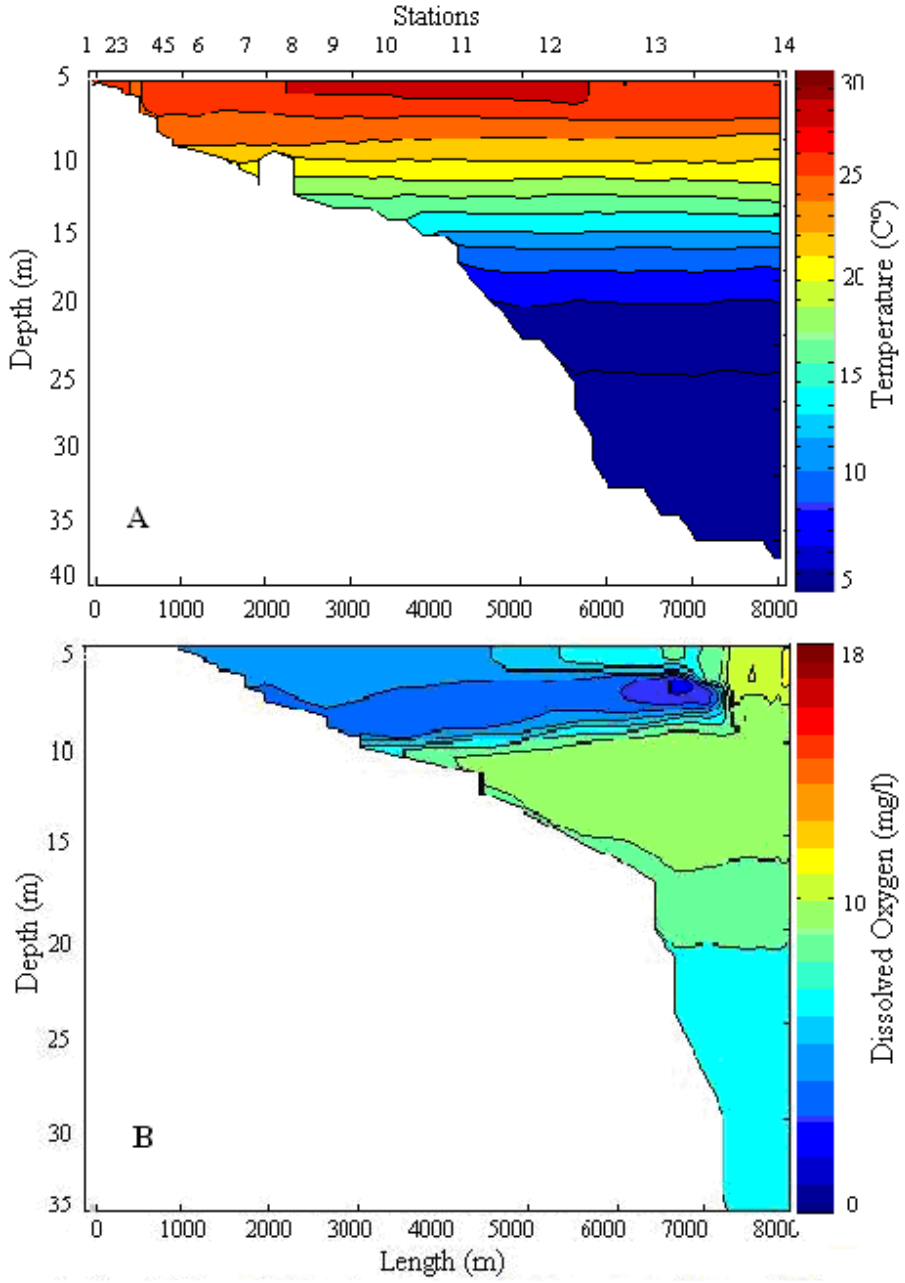
Stations
1 23 45 6 7 8 9 10 11 12 13 14
Depth (m)
5 10 15 20 25 30 35 40
A
0 1000 2000 3000 4000 5000 6000 7000 8000
Temperature (C°)
30 25 20 15 10 5
Depth (m)
5 10 15 20 25 30 35
B
0 1000 2000 3000 4000 5000 6000 7000 8000
Length (m)
Dissolved Oxygen (mg/l)
18 10 0

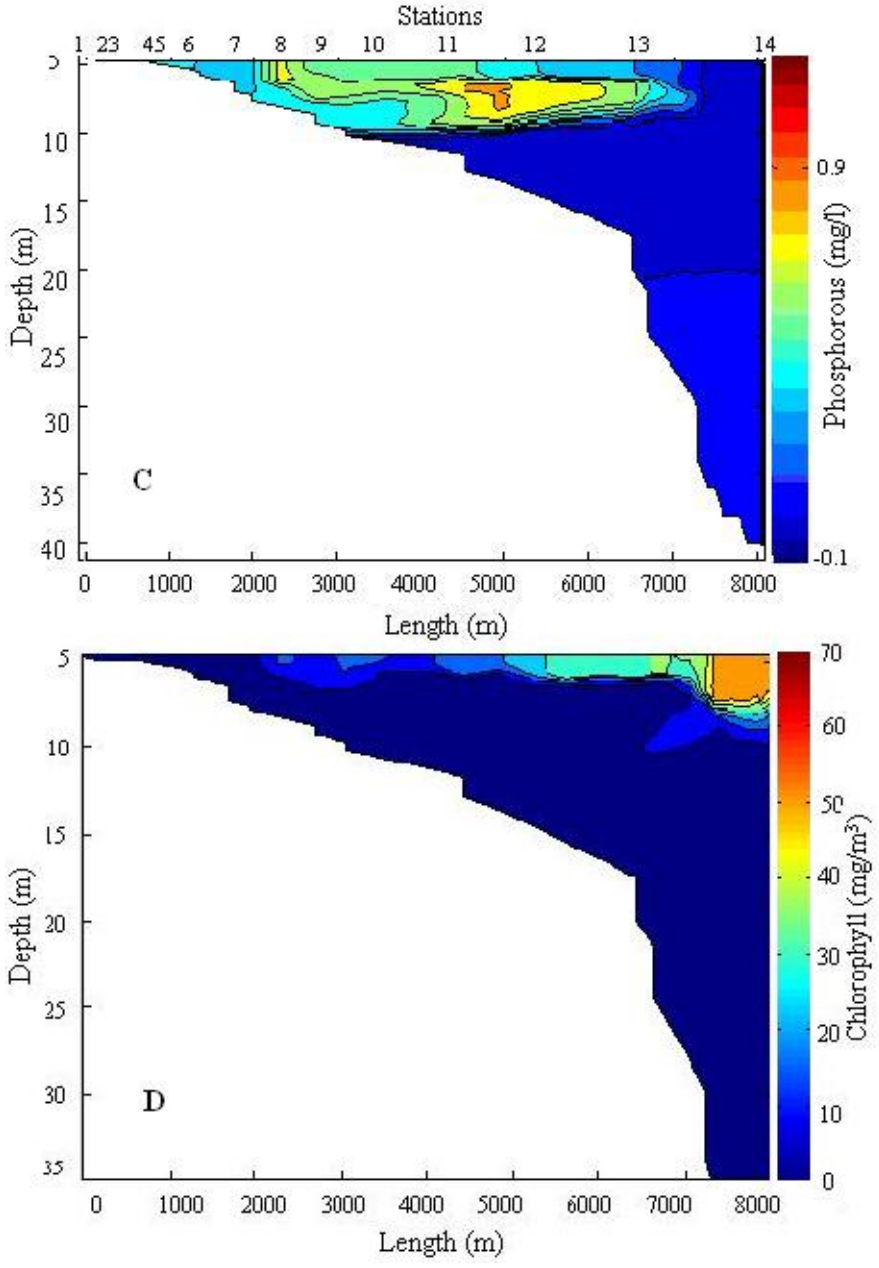


**Figure 6 : Longitudinal contour of (A) Temperature, (B) Dissolved Oxygen, (C) Phosphorous and (D) Chlorophyll following the thalweg during day 211.**

With ELCOM-CAEDYM model we can simulate how the dissolved oxygen, Phosphorus and phytoplankton response to the inflow dynamic. So this model could be considered as a good useful tool for the prediction of dissolved oxygen bloom events as well as intrusion of possible contaminants. The model also provide us with information about inflowing water distribution throughout the water column of the reservoir such information might be useful to help in such management purposes.

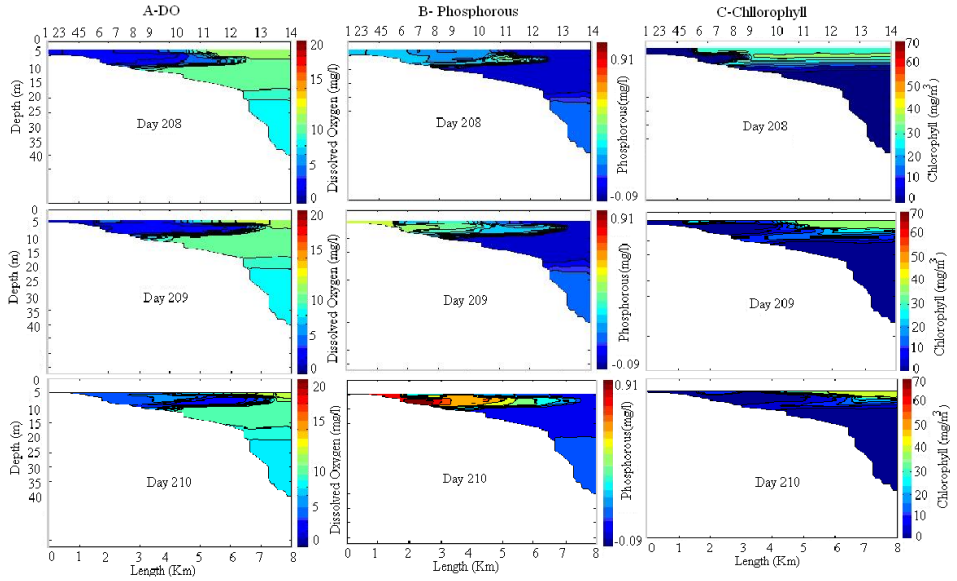


**Figure 7 : Evolution of Dissolved Oxygen, Phosphorous Vs Chlorophyll obtained with ELCOM-CAEDYM, starting from homogeneous conditions at day 206.5.**

## CONCLUSIONS

ELCOM-CAEDYM is good tool to simulate 3D hydrodynamic and water quality as it has been demonstrated in this study where river dynamic changes from overflow to interflow only due to river inflow temperature. Because, river temperature is strongly correlated with short term variations in the weather conditions and in the daily warming-cooling cycle. Such temperature variations cause changes in the river density which generates a highly dynamic inflow. This inflow dynamic enhances vertical mixing in the water column and in the in the river-reservoir interaction zone.

Also it has been noted that in the overflow situation, incoming nutrients depends on the inflow dynamic that was responsible of the apparition of algal blooms Fig. 7B.

Unfortunately, in this survey period water quality profiles as concentrations of dissolved oxygen, phosphorus and chlorophyll were not available in order to compare simulated results with field ones. This study for monitoring hydrodynamic and water quality in Sau Reservoir in Catalonia, Spain that might be used as reference study for further investigation in Algerian reservoirs.

## REFERENCES

Akiyama J., Stefan G.H. (1984). Plunging flow into a reservoir: theory. J. Hydraul. Eng. ASCE, 110, 484–489

Alavian V., Ostrowski P. (1992). Use of density current to modify thermal structure of TVA reservoirs. J. Hydraul. Eng. ASCE, 118, 5, 688–706.

Alavian, V., Jirka, G.H., Denton, R.A., Johnson, M.C., Stefan, H.G., 1992. Density Current Entering Lakes and Reservoirs, J. Hydraul. Eng. ASCE, 118, 1464–1489.

Armengol J., Toja J, Vidal A. (1994). Seasonal rhythm and secular changes in Spanish reservoirs, in: R. Margalef (Ed.), Limnology Now: A Paradigm of Planetary Problems, Elsevier Science, Amestrdam, , pp. 237–253

Armengol J., Gracia M., Comerma M., Romero J., Dolz M., Roura B.P., Han A., Vidal K., Simek K. (1999). Longitudinal processes in canyon type reservoirs: The case of Sau (N.E. Spain), in: J.G. Tundisi, M.Straskraba (Eds.), Theoretical Reservoir Ecology and its Applications, Backhuys Publishers, Leiden, pp. 313–345.

Ford D.E., Johnson M.C., Monismith S.G. (1980). Density inflows to DeGray lake, Arkansas. In: Second international symposium on stratified flows, IAHR, Trondheim, Norway

Hipsey M.R.J., Romero R., Antenucci J.P., Hamilton D. (2005) Computational Aquatic Ecosystem Dynamic Model: CAEDYM v2 Science Manual, Center for Water Research, University of Western of Australia, Perth.

Hodges B.R. (2000). Numerical techniques in CWR-ELCOM. Technical report, Centre for Water Research, University of Western Australia, Nedlands, Western Australia, 6907. Reference WP 1422-BH.

Hodges B.R., Dallimore C. (2006). Estuary, Lake and Coastal Ocean Model: ELCOM v2.2 Science Manual. Centre for Water Research. University of Western Australia

Imberger J. (2001). Characterizing the dynamical regimes of a lake 6th Workshop on physical Process in Natural Waters University of Girona: 77-92.

Laval B., Hodges B.N. (2000). The CWR Estuary and Lake Computer Model ELCOM. User Manual, Centre for Water Research, University of Western Australia.

Romero J.R., dallimore C.P., Antenucci J.P., Hamilton D.P., Imberger J., Hora D.A., Deen A. (2007). Application of 1D and 3D Hydrodynamic Models Coupled to an Ecological Model to Two Water Supply Reservoirs. Sydney Catchment Authority, Penrith, NSW 2750: 307-312

Savage S.B., Brimberg J. (1975). Analysis of plunging phenomena in water reservoirs, J. Hydraul. Res., 13, 2, 187–204.

Schladow G.S., Hamilton D.P. (1997). Prediction of water quality in lakes and reservoirs: Part I- Model description. Ecological Modelling, 96: 91-110.

Takkouk S., Casamitjana X. (2016). Application of the DYRESM–CAEDYM model to the Sau Reservoir situated in Catalonia, Spain. Desalination and water treatment journal, Vol.57, Issue 27, 12453-12466.